Meas. Sci. Technol. **9** (1998) 686–691. Printed in the UK PII: S0957-0233(98)82022-5

A new amplifier design for fast low-noise far-infrared detectors using a pyroelectric element

R N Schouten

Faculty of Applied Physics, Delft University of Technology, PO Box 5046, 2600 GA Delft, The Netherlands

Received 20 February 1997, accepted for publication 6 January 1998

Abstract. A new concept for pyroelectric detector circuits with a flat signal bandwidth of 10 kHz or more is reported. It leads to signal-to-noise ratio improvement by a factor of 50 compared with commercially available fast pyroelectric detector circuits. The approach is also showing a larger bandwidth, ease of implementation and noise improvement compared with add-on frequency-compensating circuits for bandwidth enlargement. A demonstration circuit has been built using a low-cost pyroelectric detector element. The design can be used for amplification of other high-impedance sources too.

1. Introduction

Pyroelectric detectors can be used to monitor 'optical' signals for wavelengths from the nanometre to the millimetre range. Operation of these detector elements is at room temperature and response times can be as short as nanoseconds.

A pyroelectric detector can be regarded as a capacitor with temperature-dependent polarization; an optical signal causes a temperature change that gives rise to a displacement current [1, 2]. Because of thermal relaxation this will only work for AC signals from approximately 0.1 Hz up (the thermal time constant). Major drawbacks are a low sensitivity combined with a large capacitance. The output current as a function of the incident optical power is about a million times less than that of a photodiode and capacitance values are in the range 2–200 pF. Typical values for a 2 mm diameter element are a sensitivity of 1 μA W^{-1} and a capacitance of 30 pF. Amplification of the detector signal consists of current-to-voltage conversion. For applications monitoring optical pulse shapes this conversion has to be frequency independent in the bandwidth of interest, usually 10 kHz or more, starting from the 0.1 Hz set by the thermal time-constant. The detector capacitance is the upper frequency-limiting factor (the electrical time constant).

Four different methods of signal amplification, three existing ones and a new one, are briefly introduced and then evaluated regarding their signal-to-noise ratio and bandwidth specifications. The evaluation is focused on circuits having a flat signal bandwidth and on the implementation problems limiting their practical use. Calculated and measured data are presented showing a significant improvement in ease of implementation and noise performance for the new amplification method. To compare the noise of the different detector circuits, the so called noise equivalent power (NEP) (W Hz$^{-1/2}$) is used, to express the output noise as an equivalent detectable optical input power for a given bandwidth.

2. Evaluation of pre-amp designs

Four amplifier designs, including one new one, will be evaluated in terms of noise performance, bandwidth and related implementation problems. Each amplifier type is described in a separate subsection of this section. Existing types (figure 1) are called voltage mode, current mode and integrating mode amplifiers. The new design is called an integrating/differentiating mode amplifier. The detector element can be modelled as a current source in parallel with a capacitance. Assuming a detector sensitivity of S (A W^{-1}) and a current-to-voltage conversion using a resistor R, the lowest noise floor, expressed as an optical power, will be

$$\text{NEP} = \text{resistor noise/voltage responsivity} = (4kTBR)^{1/2}/SR \quad (1)$$

where $k = 1.38 \times 10^{-23}$ J K^{-1}, T is the temperature in Kelvins and B is the bandwidth in hertz.

This leads to the conclusion that a *higher* resistance value gives a *lower* NEP (assuming noiseless electronics). In table 1 this theoretical value is compared with values realized for each type of amplifier, assuming a *flat signal bandwidth* of 10 kHz. The electronic circuits create added (frequency-dependent) noise. To be able to compare realized detector circuits with frequency-dependent NEP values the integrated NEP over the full 10 kHz is given (in

0957-0233/98/040686+06$19.50

Table 1. A comparison of NEPs for the four different amplification circuits.

Mode	Circuit elements	NEP integrated 10 kHz (W)		NEP spot 10 kHz (W Hz$^{-1/2}$)	
		Calculated	Realized	Calculated	Realized
Voltage (VM)[a]	R = 500 kΩ	1.6×10^{-5}	2.6×10^{-5}	1.6×10^{-7}	2.6×10^{-7}
Current (CM)[b]	R = 100 MΩ C_f = 0.2 pF	1.2×10^{-6}	4.8×10^{-5}	1.2×10^{-8}	$> 4.8 \times 10^{-7}$
Integrating (IM) plus compensation[c]	R = 50 GΩ	5.1×10^{-8}	1.5×10^{-6}	5.1×10^{-10}	4×10^{-8}
Integrating/differentiating (ID)[d]	R = 1 GΩ	3.6×10^{-7}	4.7×10^{-7}	3.6×10^{-9}	4.7×10^{-9}

[a] Molectron PI-72 ultra-low-noise detector, manufacturer's data.
[b] Molectron PI-42 low-noise detector, manufacturer's data, NEP 10 kHz spot not specified for 10 kHz bandwidth application.
[c] GEC-Marconi PLT522, manufacturer's NEP specifications for the IM stage and assuming an ideal noiseless added frequency-compensating amplifier [3].
[d] New ID detector data determined by gain measurement at 670 nm with a calibrated source, verified by detector gain specification and circuit current gain measurement. Output spectral noise measured on a Stanford SR760 spectrum analyser. For all detector elements S = 1.1 μA W^{-1}, C_d = 30 pF and diameter 2 mm. The signal bandwidth was 10 kHz. NEP values were calculated using equation (1), assuming noiseless electronics.

Watts) together with the NEP at a spot frequency of 10 kHz (in W Hz$^{-1/2}$). The magnitude of the difference between the calculated and realized values indicates implementation problems.

In table 2 the influence of additional noise from the electronics is illustrated. Expressions are given for the bandwidth, responsivity, output noise and NEP; the contributions from amplifier voltage noise (E_n) and current noise (I_n) are included explicitly. In Figure 2 the resulting noise and responsivity curves are shown for the new design and compared with those for the existing circuits implemented for an example bandwidth of 10 kHz. The four amplifier designs, including the new one, will be discussed in relation to this theoretical and practical performance, showing that the new design offers far better results.

2.1. The voltage mode amplifier

The detector current flows into R, creating a voltage buffered by the FET. The signal bandwidth is set by RC_d. For a typical FET buffer the noise contributions E_n and I_n can be neglected for R values between 10 kΩ and 1 GΩ. Creating a 10 kHz bandwidth for a 30 pF element results in a 500 kΩ resistor for R. In this region the NEP is determined by equation (1) and will be constant over the signal bandwidth. There is however no room for NEP improvement insofar as the value for R is already set by the desired bandwidth (see figure 2(c)).

2.2. The current mode amplifier

The detector current flows into R. Because R is in the feedback of a high-gain amplifier, a virtual low-impedance node is present at the detector pin, enlarging the signal's bandwidth. Here the bandwidth is limited by the stray capacitance C_f across R. For a 10 kHz bandwidth using $R = 1$ GΩ, C_f must be lower then 0.016 pF, which is difficult to achieve. The minimum value for C_f that can be realized sets the highest value for R. A second problem is the amplification of the voltage noise E_n by a factor $1 + Z_{feedback}/Z_{detector}$. The resulting frequency-dependent amplifier noise gain, given by the term G_ω in table 2, is set by the time constant RC_d. This can cause a rising NEP (spot) with frequency within the signal bandwidth (depending on implementation, see figure 2(d)), degrading results and thus also limiting the useful maximum value for R. This effect is the origin of the difference between theoretical and realized results for the PI-42 detector given in table 1. The implementation problems described above have also been reported in the literature [2] and by manufacturers [3, 4, 6].

2.3. The integrating mode amplifier, combined with a frequency-compensation amplifier

For the integrating mode R is chosen much larger than that which is given by the bandwidth demands, resulting in a better noise performance but a smaller signal bandwidth. This circuit is not suited for monitoring pulse shapes because it exhibits a $1/f$ frequency response. Pulses with a length $\tau \ll RC_d$ and power P are integrated and the capacitance C_d is charged to a voltage step $PS\tau/C_d$. This forms the output signal of the integrating mode amplifier. The fact that ω is present in the gain *and* in the output noise expressions (table 2) leads to an important conclusion. The NEP as a function of the frequency is *constant* until the E_n^2 term dominates the output noise (as the gain drops, the noise drops). As suggested in [3], a frequency-compensating amplifier could be used to compensate for the $1/f$ response. The implementation of such a set-up is based on a 10 kHz signal bandwidth using a GEC-Marconi PLT522 2 mm diameter element with integrated FET follower and a resistor R of 50 GΩ [4]. The specifications of the PLT522

Table 2. Expressions for the bandwidth, responsivity and output noise of amplification modes.
NEP = output noise/responsivity (W $Hz^{-1/2}$). E_n and I_n are the voltage noise and current noise of the amplifier. $G_\omega = 1 + \omega RC_d$ is the amplifier noise gain. $Z_\omega = R/(1 + \omega^2 R^2 C_d^2)^{-1/2}$ is the parallel impedance of C_d and R. D_ω is the differentiator gain. D_n is the differentiator noise voltage. G_F is the gain of the FET to the differentiator input.

Mode	Bandwidth (Hz)	Responsivity (V W^{-1})	Output noise (within bandwidth) (V $Hz^{-1/2}$)
VM	$1/(2\pi RC_d)$	SR	$(4kTR + E_n^2 + I_n^2R^2)^{+1/2}$
CM	$1/(2\pi RC_f)$	SR	$(4kTR + E_n^2G_\omega^2 + I_n^2R^2)^{+1/2}$
IM		$S/(\omega C_d)$	$[(4kT/R)Z_\omega^2 + E_n^2 + I_n^2Z_\omega^2]^{+1/2}$, $\tau \ll RC_d$
ID	$D_\omega/(2\pi RC_d)$	SR	$D_\omega[(4kT/R)Z_\omega^2 + E_n^2 + I_n^2Z_\omega^2 + D_n^2/G_F^2]^{+1/2}$

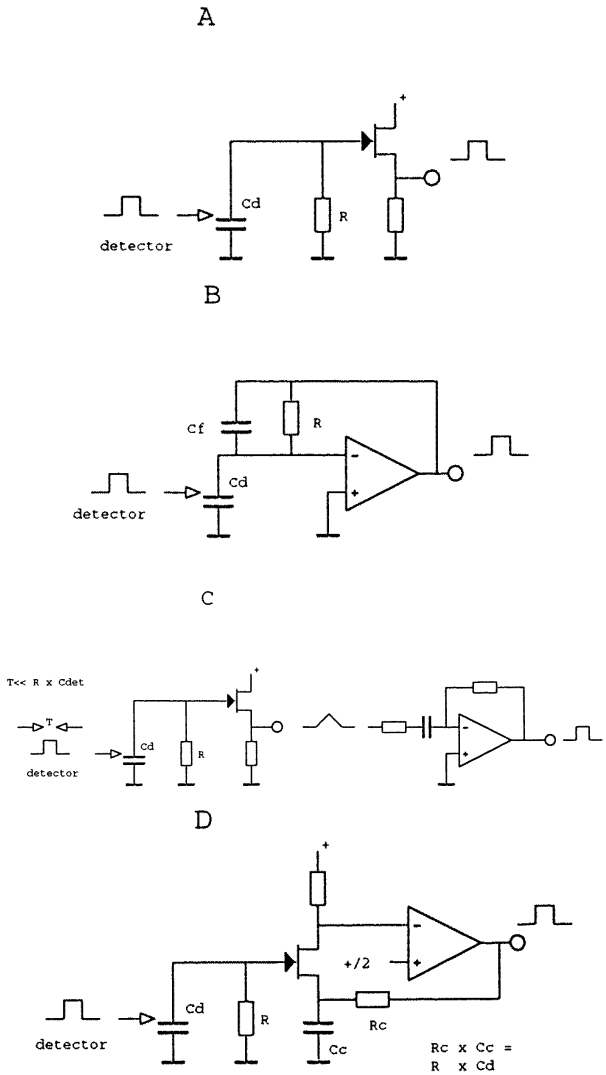

Figure 1. (a) Voltage mode (VM), (b) Current mode (CM), (c) Integrating mode (IM) plus compensation (IMC) (d) Integrating/differentiating mode.

device show that E_n^2 is dominating from 100 Hz up [3], resulting in degradation of the noise performance in a 10 kHz signal bandwidth (see table 2 and figure 2(d)). It has to be noted that the noise contribution of a compensating amplifier, described in [3], still has to be added; in this evaluation it is assumed to be zero. The dominating E_n^2 contribution at frequencies above 100 Hz is common for all commercially available elements with an integrated FET follower as a result of the need for FETs with low input currents when using R values of 10 GΩ or higher.

2.4. The (new) integrating/differentiating amplifier

In the VM and CM designs the limitations described above leave no room for improvement of the NEP via enlargement of R. Therefore the design starts with choosing R larger, giving an integrating network RC_d just like that of the integrating mode detector. Its output signal is differentiated using a design that does not give a significant noise contribution (figures 2(a) and (b)). The discrete front-end FET forms a gain stage (not a follower) from which a better noise performance is obtained. Using a low-voltage noise discrete junction FET also improves the noise performance at frequencies above 100 Hz (see figures 2(c) and (d)). The original bandwidth F_1 set by the value of R is increased to a value F_2, without degrading the NEP. The resulting NEP (spot) is frequency independent. Above F_2 the output noise is dominated by E_n. The value of R can be in the giga-ohm range, because its value does *not* set the signal bandwidth; the signal bandwidth is only limited by the finite gain of the differentiator stage.

Stray capacitances of R and of the FET in the picofarad range can be tolerated because they are parallel to $C_{detector}$. The remaining compensating time constant network in the op-amp stage (R_cC_c) is a low impedance (kilo-ohm) configuration, thus avoiding stray-capacitance problems.

From the expressions in table 2 it follows that differentiator noise can be neglected if $G_F > D_n/E_n$. This condition is easily satisfied (see the circuit description). To achieve constant gain within the signal bandwidth, the impedance drop of Z_ω (20 dB per decade above F_1) is compensated by the differentiator gain D_w. In a similar way, the voltage noise drop of Z_ω together with the differentiator gain results in a flat frequency spectrum for the output noise. This is valid as long as E_n is smaller than the thermal noise from Z_ω, that is for $F < F_2$. So, up to F_2, the NEP (spot) is constant and determined only by R, as in equation (1).

An additional increase of bandwidth obtained by extending the differentiator gain beyond F_2 is still giving improved NEP results compared with existing designs (figure 2(c)). In that situation, above F_2 the NEP will rise with 20 dB per decade. Existing designs exhibit a 10 dB

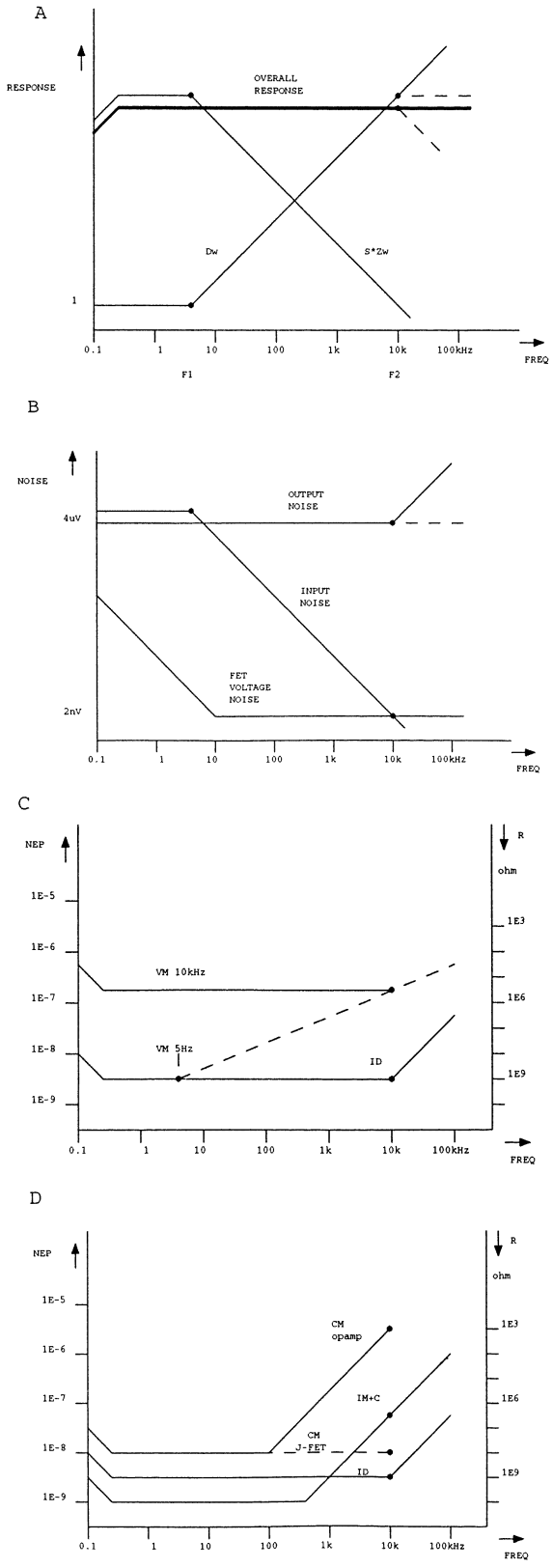

Figure 2. (a) Gain stages of the ID mode; the broken line is the 10 kHz bandwidth limit (in the example and figure 3).
(b) Noise levels of the ID mode, the broken line is the 10 kHz bandwidth limit (in the example and figure 3).
(c) A NEP (spot) comparison of VM and ID modes.
(d) A NEP (spot) comparison of CM, IM ID modes.

per decade rise in NEP if the bandwidth is enlarged by lowering R (1) and so the advantage of the ID method will gradually disappear for higher frequencies.

3. Conclusions

(i) Compared with the voltage mode detector (see figure 2(c)) this new method yields an improvement of the NEP (integrated) by a factor $(F_2/F_1)^{1/2}$, for signal frequencies up to F_2. Here $F_1 = (2\pi RC_d)^{-1}$ and $F_2 = F_1(4kTR)^{1/2}/E_n$. Given the values of the implementation example, this leads to a NEP improvement by a factor of 44. These low NEP values could have been obtained for the VM detector only by lowering the bandwidth to 5 Hz using 1 GΩ (see figure 2(c)). When extending differentiator action for the ID mode above F_2, a (gradually decreasing) improvement in NEP is available up to a frequency $F_3 = F_2(F_2/F_1)^{1/2}$.

(ii) In figure 2(d) a comparison with the current mode detector is illustrated. Theoretically the NEP of the current mode detector can be as low as that of the IM detector, but it leads to problematic constraints such as the need to lower the total stray capacitance across $R_{feedback}$ to less then 0.016 pF for a 10 kHz bandwidth. Practical implementation in commercially available detectors shows that, even when a stray capacitance as low as 0.2 pF is achieved (PI-42, $R_f = 100$ MΩ and bandwidth 10 kHz), the amplified op-amp noise becomes dominant. This latter problem could be reduced by adding a discrete low-noise FET in the loop (see figure 2(d), broken curve). However, stability problems could arise from such a composite amplifier with overall feedback to the input capacitor C_d. The elegance of the new method is the avoidance of these problems by using compensation instead of high impedance feedback to the input node. As shown in table 1 (the 10 kHz example) improvements in NEP by a factor of 50 compared with commercially available circuits can be made.

(iii) Compared with type 3 (an integrating detector combined with a compensation amplifier), this new solution has several advantages. The noise performance is improved because of the gain of the discrete FET with better noise specifications. Even when assuming a noiseless frequency-compensating amplifier for the IM mode using 50 GΩ, the new ID mode exhibits a better calculated and realized integrated NEP in a 10 kHz bandwidth using only 1 GΩ. The NEP at spot frequencies below 100 Hz is still larger for the new ID mode but at higher frequencies the NEP (spot) for the IM plus compensating amplifier rises to a factor of ten above that of the ID mode. This accounts for the improvement in integrated NEP of the new ID circuit. FETs with a low leakage current such as are needed in a 50 GΩ application will tend to have a high voltage noise and a low gain [3]. Using only 1 GΩ for R decreases input current problems and temperature instability [1, 2] making it possible to use a lower voltage noise FET type with higher gain. Because the FET voltage noise is the dominating factor above 100 Hz, this reduces the noise for the 10 kHz application. The FET gain lowers the specified gain bandwidth for the op-amp stage and thus enlarges the obtainable bandwidth. Using only 1 GΩ also

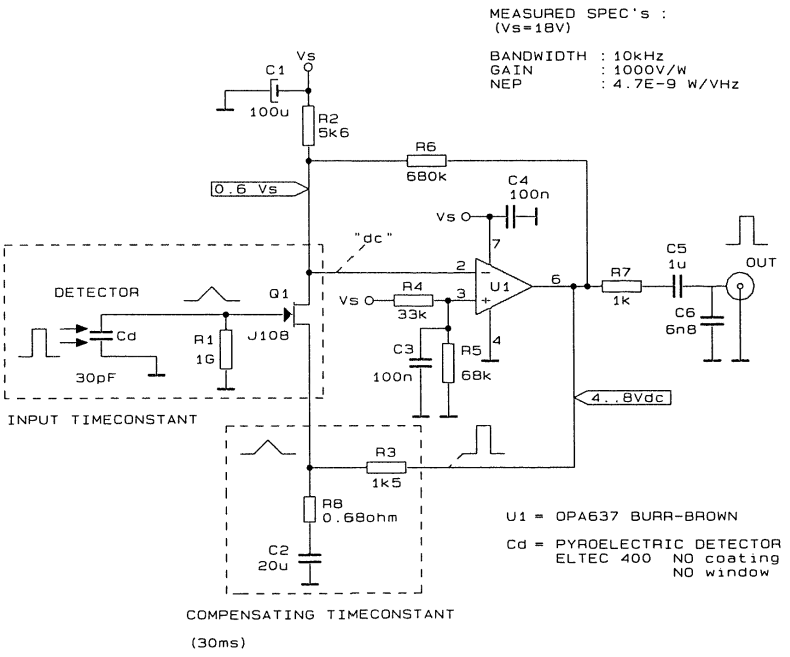

Figure 3. The 10 kHz bandwidth ID mode pyroelectric detector amplifier.

sets the starting point for the differentiating action at 5 Hz, whereas for the IM mode this would be 0.1 Hz. For the IM mode this would result in a differentiator gain of 10.000 at 10 kHz, giving implementation problems. The cascode configuration for the FET in the new ID mode eliminates excessive input capacitance resulting from the Miller effect that would appear if one were using a standard FET common source amplifier [3].

4. Implementation

Two basic designs for the implementation of the integrating/differentiating approach are shown. Figure 1(d) shows the most simple solution; a more detailed circuit is given in figure 3. In a slightly changed design, see figure 4, the detector is placed in a boot-strap configuration to enlarge the bandwidth without further increasing the differentiator gain. This boot-strap configuration lowers the time constant RC_d by positive feedback. It should be noted that the boot-strap configuration does not improve the NEP because the FET noise is coupled back to the input. Implementation is done only to lower the constraints on the differentiator circuit. Using the design shown in figure 4 improvement in integrated NEP by a factor of 25 (compared with the VM design) was achieved for a 100 kHz bandwidth detector.

5. Calculations and circuit description

Using the basic design of figure 1(d), the circuit shown in figure 3 has been built and tested. The design parameters were the following. The detector had a capacitance $C_d = 30$ pF and a sensitivity $S = 1.1$ uA W^{-1} (ELTEC 400 specifications). R was 1 GΩ and the thermal noise voltage was 4 μV Hz$^{-1/2}$.

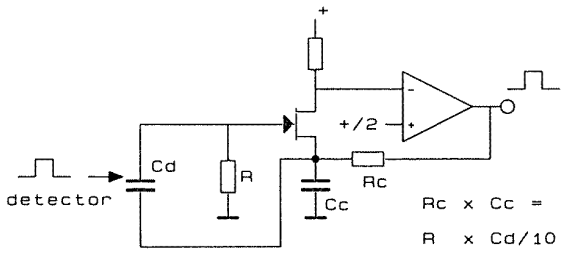

Figure 4. The integrating/differentiating mode, including the detector's boot-strap configuration.

The noise voltage of the FET was 2nV Hz$^{-1/2}$ and the FET capacitance was < 3 pF (parallel to C_d).

5.1. Calculations

The uncompensated integrator bandwidth is $F_1 = (2\pi RC_d)^{-1} = 5$ Hz. For signals up to this frequency the gain is set by SR. At frequencies above F_1, the gain drops with 20 dB per decade (a first-order response). To create a flat frequency response, the differentiator has to operate from frequency F_1 up, so the FET-stage output signal and noise will be amplified with 20 dB per decade starting from 5 Hz (figure 2(a)).

The noise voltage from the input section (R parallel to C_d) starts at the thermal noise level of R (4 μV Hz$^{-1/2}$), but, from F_1 up, this declines with 20 dB per decade because of the impedance of C_d in parallel (figure 2(b)). The FET noise voltage as a function of the frequency is fairly constant at 2 nV Hz$^{-1/2}$; the increasing $1/f$ noise below 100 Hz is still negligible compared with the value

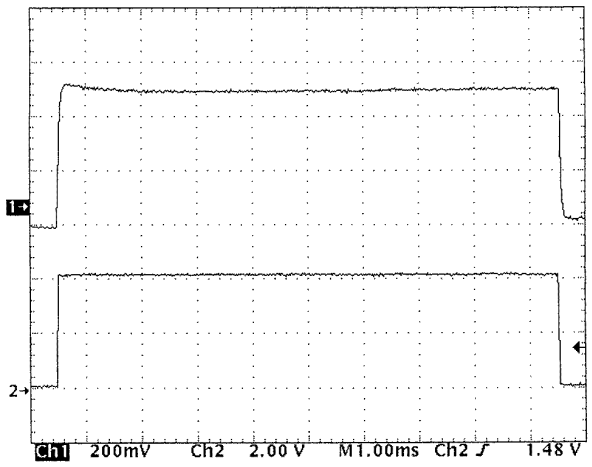

Figure 5. The output pulse (upper trace, 1 mS per division) of the circuit from figure 3 as a result of an optical input signal (lower trace).

4 μV Hz$^{-1/2}$ due to R. This leads to the conclusion that the FET noise will dominate for frequencies above $F_2 = (4\ \mu\text{V}/2\ \text{nV}) \times 5\ \text{Hz} = 10$ kHz (figure 2(b)). In order to operate the circuit up to F_2, the differentiator gain has to be $F_2/F_1 = 2000$ at frequency F_2, so an op-amp with gain bandwidth larger than 20 MHz is needed for a 10 kHz signal bandwidth implementation.

5.2. The circuit description

An optical pulse will be converted into a current flowing in the parallel circuit of R_1 and $C_d + C_{stray} + C_{fet}$. FET Q_1 buffers the voltage across R_1 and generates a current in its drain–source circuit. C_{stray} can be below 1 pF and the influence of C_{fet} is reduced by the design, as explained below, so both can be neglected.

Op-amp U_1 is DC biased at its positive input and has $R_3 - Q_{1source} - Q_{1drain}$ as its main feedback path (R_6 is only gain limiting). The signal current generated by the FET will therefore be compensated by the op-amp to keep its negative input at the given DC bias level. For infinite op-amp gain, the resulting alternating current through the FET will be close to zero, because the AC source voltage will equal the AC gate voltage. This cascode circuit keeps the FET capacitance from loading the detector element.

The op-amp feedback path contains a time constant R_3C_2 equal to the time constant of the input circuit $R_1(C_d + C_{stray} + C_{fet})$. The resulting output signal of the circuit will then have a flat frequency response up to the gain limit set by R_8/R_3. C6 is an (optional) output filter for out-of-band noise. The measured output pulse (figure 5, upper trace) from an optical input pulse (figure 5, lower trace) shows the effectiveness of the compensation.

5.3. Practical considerations

As noted before, the voltage noise of the FET limits the possible improvement in NEP. In the usual detectors with integrated FETs, voltage noise is high, so here a passive detector element followed by a discrete low-noise voltage (< 2 nV) FET is used. The voltage noise of the op-amp in this design makes a lesser contribution, because of the gain ($G_F = R_2/R_3$) of the FET in its feedback path. A voltage noise below 8 nV will suffice. For the op-amp, a high-speed (60 MHz) low-noise (4.5 nV) FET op-amp is used. Capacitor C_2 in the compensating network has to be a low-inductance, low-series resistance type (no electrolytic) because at 10 kHz its impedance should be well below R_3 in order to preserve the compensation curve needed. The power supply can be a battery or other low-noise supply, stability is not needed; the circuit gain varies by 20% for a supply range 15–25 V.

6. Results and conclusion

For a 10 kHz bandwidth pyroelectric FIR detector using a 2 mm element the new ID mode circuit offers an improvement in integrated NEP by a factor of 50 (VM mode) to 100 (CM mode) compared with commercially available solutions. The realized circuit offers a NEP (4.7×10^{-9} W Hz$^{-1/2}$) close to the theoretical value (3.6×10^{-9} W Hz$^{-1/2}$) when working up to a bandwidth of 10 kHz, showing the absence of implementation problems involved with existing designs like the IM mode detector combined with an additional frequency-compensating amplifier. For bandwidths below 100 Hz the latter still offers the best possible noise performance.

References

[1] Whatmore R W 1986 *Rep. Prog. Phys.* **49** 1335–86
[2] Porter S G 1981 *Ferro-electrics* **33** 193–206
[3] GEC-Marconi Pyroelectric sensors application notes
[4] GEC-Marconi Pyroelectric detectors product handbook
[5] Molectron Datasheets PI-72, PI-42 detectors
[6] ELTEC Datasheet type 40612 current/voltage mode detector